



## Examination of the activity and durability of PEMFC catalysts in liquid electrolytes

Ikuma Takahashi<sup>a</sup>, Shyam S. Kocha<sup>b,\*</sup>

<sup>a</sup> Fuel Cell Laboratory, Nissan Research Center, Yokosuka, Japan

<sup>b</sup> Fuel Cell Laboratory, Nissan Technical Center North America, 39001 Sunrise Drive, Farmington Hills, MI 48331, USA

### ARTICLE INFO

#### Article history:

Received 10 March 2010

Received in revised form 16 April 2010

Accepted 16 April 2010

Available online 22 April 2010

#### Keywords:

RDE

Platinum catalyst

Polymer electrolyte membrane (PEM) fuel cell

Activity

Durability

### ABSTRACT

Widespread research in the field of fuel cells necessitates easily verifiable and reproducible benchmarks for characterizing properties such as electrochemical area (ECA), oxygen reduction reaction (ORR) specific and mass activity ( $i_s$ ,  $i_m$ ) as well as durability of electrocatalysts. *Ex situ* characterization of electrocatalysts deposited as thin-film rotating disk electrodes (TF-RDE) in liquid electrolytes as well as in their original dry powder state has been conducted. Commercially available Pt on carbon support (Pt/C) catalyst serving as a baseline benchmark and heat treated Pt/C and Pt-alloy/C catalysts were investigated as examples of higher activity and durability materials. A detailed description of the preparation and optimization of catalyst inks, measurement protocols, and analysis of ORR kinetic parameters and durability rates are provided to form a basis for consistent screening and benchmarking of new and improved catalysts for proton exchange membrane fuel cells (PEMFCs). Preparation of highly-dispersed ink slurries formulated using various water–isopropanol mixtures and deposited as TF-RDEs were demonstrated to significantly affect the magnitude of measured ECA and activity. The ECA,  $i_s$  and  $i_m$  for the baseline Pt/C were determined to be  $100 \text{ m}^2 \text{ g}^{-1}$ ,  $292 \mu\text{A cm}^{-2}_{\text{Pt}}$  and  $266 \text{ mA mg}^{-1}_{\text{Pt}}$  in  $0.1 \text{ M HClO}_4$  at  $25^\circ\text{C}$  and  $10 \text{ mV s}^{-1}$ . Strong adsorption of anions on Pt/C in sulfuric acid was shown to have a deleterious effect on its activity and durability. Related ORR kinetic parameters such as the activation energy ( $\Delta H = 38 \text{ kcal mol}^{-1}$ ) as well as the experimental reaction order ( $m \sim 0.75$ ) with respect to oxygen were determined to provide a basis for converting literature results to a common pressure and temperature.

© 2010 Elsevier B.V. All rights reserved.

### 1. Introduction

Proton exchange membrane fuel cells (PEMFCs) for automotive purposes have advanced to a degree where commercialization is expected to be initiated in the 2015–2020 time-frame. Platinum and Pt-based alloy nanoparticles dispersed on a carbon black support (coated onto membranes to form membrane electrode assemblies (MEAs)) continue to be the most common catalyst materials for application in practical PEMFCs for automotive use. One of the major impediments to automotive PEMFC commercialization is the high intrinsic cost of Pt ( $\$50 \text{ g}^{-1}$ ). State-of-the-technology MEAs employ a total Pt loading of about  $0.40 \text{ mg}_{\text{Pt}} \text{ cm}^{-2}$  that amounts to  $\sim 30 \text{ g Pt per } 100 \text{ kW stack}$ . About  $0.05 \text{ mg}_{\text{Pt}} \text{ cm}^{-2}$  of Pt catalyst is applied to the anode (with minimal overpotential losses) for the fast hydrogen oxidation reaction (HOR) and about  $0.35 \text{ mg}_{\text{Pt}} \text{ cm}^{-2}$  is applied to the cathode (with  $\sim 400 \text{ mV}$  incurred losses) for the slow four-electron ( $4e^-$ ) oxygen reduction reaction (ORR). In order to meet the cost goals for commercialization of PEMFCs, a lower-

ing of the Pt loading by a factor of 4–10 is necessary. Pathways to accomplish this target are through the use of higher activity Pt-alloy catalysts, core–shell catalysts that employ Pt only on the surface of nanoparticles and extended thin-film catalysts that possess an intrinsic high specific activity. Improving the mass-transport in PEMFCs with resultant operability at higher current densities (from 1 to  $3 \text{ A cm}^{-2}$ ) can also contribute to the lowering of total Pt catalyst used in stacks. In addition to the requirement of improved activity, the catalyst is also required to endure about 5000 h/10 years in a PEMFC stack while being subjected to harsh automotive conditions of idling, load cycling, start–stop cycles, freeze–thaw cycles, etc., with  $<10\%$  loss in performance at peak power. Thus, the search for a high activity/high durability Pt-based catalyst that can meet the cost target for automotive commercialization is an extremely active field of research and development in laboratories throughout the world [1–4].

As a result of the intensive research conducted in industry, academia and government laboratories in the preparation of new and improved Pt-based catalysts, a large number of potential candidates in very small quantities ( $<0.5 \text{ g}$ ) are typically prepared in lab-scale set-ups. Hence a reliable, low-cost and efficient way of screening the activity and durability of these new sample catalysts

\* Corresponding author. Tel.: +1 3032753284; fax: +1 3032753840.

E-mail address: [shyam.kocha@yahoo.com](mailto:shyam.kocha@yahoo.com) (S.S. Kocha).

is indispensable. Although high-throughput and combinatorial screening [4–6] of novel non-supported metal–alloy catalysts have been attempted with limited success, a typical method to measure improvements in activity and durability of new dispersed catalysts has been its initial screening in half-cell liquid electrolyte set-ups using thin-film rotating disk electrodes (TF-RDEs). TF-RDEs are prepared using supported catalysts identical to that used in PEMFCs and can provide a reasonably realistic and practical assessment of catalyst activity [7–10]. Successful catalyst candidates that pass the screening tests for activity and durability in half-cells can be subsequently scaled up to produce larger quantities and then tested under more realistic conditions in subscale fuel cells having an active area of 25–50 cm<sup>2</sup> after ink and electrode optimization. The final step is usually the testing of full size MEAs (100–400 cm<sup>2</sup>) in PEMFC short-stacks assembled using 15–30 individual cells.

A survey of the literature [7,9,11] shows that the measurement of ORR activity of Pt/C and similar catalysts are carried out under a variety of different conditions that renders it difficult to normalize, compare and hence benchmark to a standard. This leads to considerable inefficiencies, in that, one has to typically re-test material in order to confirm and verify results generated in different laboratories. A number of factors contribute to the wide range of catalyst activity values reported in the literature such as: the exact procedure (or experimental protocol) including pre-conditioning employed in testing, temperature, scan rate, acid type and concentration, and most importantly an absence of the detailed methods of catalyst ink and electrode preparation. The choice of acids for electrolyte has been a much debated subject [12,13]; perchloric acid has been favored recently since it has low anion adsorption on Pt [14,15] and is expected to simulate perfluorosulfonic acid (PFSA) membranes more closely than sulfuric or phosphoric acid. Nevertheless, sulfuric acid is often used for measurement of catalytic activity and reported in the literature since the use of perchloric acid can be plagued with low levels of inherent Cl<sup>−</sup> impurities [16] as well as from its decomposition during operation and over time that causes irreproducibility of results. Even with the purest HClO<sub>4</sub> acid, typically 0.1 M concentration is widely employed to limit the Cl<sup>−</sup> impurity concentration whereas 0.5 M is often used for H<sub>2</sub>SO<sub>4</sub>. Moreover, when the PFSA membranes or ionomer in MEAs degrade over time they are known to release sulfate ions that adsorb on Pt sites [17]. This results in both a loss of Pt activity due to the sulfate anion adsorption on the Pt surface and also an acceleration of Pt dissolution. Pt is known to electrochemically dissolve more readily in sulfuric acid (due to the facile formation of complexes) and thus conveniently provides an ‘accelerated test’ condition for short-term cyclic durability studies. As part of our benchmarking study, we have evaluated the ORR kinetics as well as dissolution rates of catalysts in sulfuric acid, perchloric acid and phosphoric acid.

A discrepancy exists in the values reported for ORR reaction order with respect to oxygen in acid electrolytes compared to that reported for actual PEMFCs [18–20]. The reaction order “ $\gamma$ ” at constant overpotential ( $\eta$ ) is typically invoked in RDE studies [21] whereas the reaction order “ $m$ ” at constant potential ( $E$ ) [7] is summoned in MEAs. The two reaction orders are related to each other by the expression  $\gamma = m - 0.25$ . To further complicate the results, the measurement conditions in PEMFCs are based on pseudo-steady-state data points whereas those measured in TF-RDE are based on linear sweep voltammetry (LSV). We have examined the reaction order in TF-RDEs using both LSV protocols and a pseudo-steady-state method in an attempt to elucidate the cause of discrepancies in the literature. Our objective in establishing and confirming the reaction order is to permit accurate accounting of the effect of oxygen partial pressure and temperature ( $\Delta H$ , kcal mol<sup>−1</sup>) so that ORR activity results measured under a reported set of oxygen partial pressure and temperature can be compared to a set of standard benchmarking conditions.

In this work, we have employed a commercially available (TKK, Japan) Pt/C catalyst as a benchmarking baseline case and compared a heat treated as well as a Pt-alloy catalyst to the benchmark. The original catalyst in the form of dry powder has been characterized using multiple spectroscopic methods such as X-ray diffraction (XRD) and transmission electron microscopy (TEM). The necessity and impact of optimizing the catalyst ink formulations used with TF-RDE for obtaining the peak activity for different catalysts, reproducibility of electrochemical area (ECA) and ORR activity, catalyst utilization has been reported for the first time. The effect of acid type on ORR activity and durability, key ORR kinetic parameters such as reaction order and activation energy have also been reported in an attempt to establish a rigorous baseline that may benefit the benchmarking of small quantities of newly developed catalysts by different groups.

## 2. Experimental

### 2.1. X-ray diffraction (XRD) and transmission electron microscopy (TEM)

X-ray diffraction and transmission electron microscopy are techniques that can both provide information on particle sizes below 10 nm. The two techniques differ in that XRD analysis provides information on crystallite size rather than actual particle size. XRD provides us with an estimate of particle size from volume-averaging across the sample whereas TEM gives us localized information generated from counting resulting in number-averaged results.

Catalyst powder samples were obtained from the catalyst vendor Tanaka Kikinzo Kogyo (TKK, Japan). Analysis was carried out using TEM microscope (H-9000UHR, HITACHI) operating at 300 kV and having a resolution of 0.1 nm. Histograms of particle size were constructed from micrographs by measuring the particle size for about 300 particles.

XRD analysis was performed using an X-ray diffractometer (MXP18VAHF, Mac science) operating with Cu K $\alpha$  radiation generated at 40 kV and 300 mA. Scans were carried out for  $2\theta$  values lying between 5° and 90°. Divergence slit was 1.0° and scattering slit was 1.0°. Crystallite sizes were estimated from the (1 1 1) peak using Scherrer's equation.

### 2.2. Catalyst ink preparation

Several commercially available catalysts were evaluated in this study including TEC10E50E (~46 wt.% Pt/C), TEC10E50-HT (~46 wt.% Pt/C-heat treated (HT)), as well as an alloy catalyst TEC36E52 (~46 wt.% PtCo/C). The first catalyst referred to in this paper as “baseline Pt/C” was studied in detail; the second heat treated catalyst will be referred to as Pt/C-HT and was chosen as an ideal candidate for longer duration tests due to its enhanced durability (lower Pt dissolution); finally the third catalyst referred to as PtCo/C was chosen to represent an example of a catalyst with improved activity and durability. Identical weight percent catalysts were chosen to maintain a consistent electrode film thickness on the electrodes.

Catalyst powders, ultra pure water (Milli-Q water, Milli-Q Co. Ltd.) and isopropanol (Wako Pure Chemical Industries) as well as 5 wt.% Nafion dispersion solution (Wako Pure Chemical Industries) were mixed using ultrasonic agitation for 30 min. The ratio of water and isopropanol (IPA) added to catalyst ink was varied so as to obtain the best dispersion and the highest electrochemical area (ECAs) from cyclic voltammograms (CVs). Nafion ionomer loading was maintained extremely low since its function was only to glue or hold the catalyst particles together atop the electrode and prevent its flaking off during high speed rotation.

One of the optimal ink formulations is presented here to facilitate reproduction of the results by those interested in benchmarking. 18.5 mg of (46 wt.% Pt/C) TEC10E50E is weighed and then mixed with 19 mL of DI water and 6 mL of isopropanol in a measuring flask. This mixture is added to a 50 mL sample bottle along with 100  $\mu\text{L}$  of 5% Nafion solution. The sample bottle is then placed in a small ice bath and ultrasonicated for 30 min. The ink is then ready for deposition ( $10 \mu\text{L}$ ,  $17.3 \mu\text{g}_{\text{Pt}} \text{cm}^{-2}$ ) onto the GC of the TF-RDE and should result in activity measurements that meet the benchmark.

Glassy carbon (GC) electrodes were polished on a polishing pad with alumina abrasive ( $0.05 \mu\text{m}$ ) and subsequently cleaned by ultrasonication in DI water followed by rinsing in DI water.  $10 \mu\text{L}$  of the catalyst ink was subsequently deposited onto the GC electrode using a micropipette. The electrodes were dried in an oven under air atmosphere at  $40\text{--}60^\circ\text{C}$  for about 5 min (or under a trickle flow of  $\text{N}_2$  for longer periods) before being inserted in the electrochemical cell for electrochemical testing.

### 2.3. Electrochemical measurements

#### 2.3.1. Electrochemical cell set-up

A three-electrode glass cell was used in the electrochemical experiments. A rigorous cleaning procedure was employed. The glassware was first cleaned using a glassware surfactant (Sparkleen) followed by a DI water ( $18 \text{ M}\Omega \text{ cm}$ ) rinse. The glassware was then soaked in concentrated sulfuric acid overnight and rinsed in DI water. Subsequently it was soaked in a 1:1 sulfuric acid:nitric acid mixture for 4 h and again rinsed in DI water. Nitric acid may be replaced by an inorganic oxidizer “Nochromix” (GODAX Laboratories, Inc. procured in hermetically sealed pouches) in the previous step. Lastly, the glassware was boiled in DI water repeatedly with intermittent DI water rinsing to ensure minimal residual impurities. The degree of success in elimination of impurities can be estimated from the magnitude of specific activity ( $>1500 \mu\text{A cm}^{-2}$  @  $900 \text{ mV}$ ,  $100 \text{ kPa O}_2$ ) obtained for a polycrystalline Pt disk measured in the cleaned cell glassware.

Sulfuric, perchloric and phosphoric acid were used in the experiments.  $0.5 \text{ M H}_2\text{SO}_4$  was obtained from Wako Pure Chemical Industries. Double distilled, ultrapure 70% perchloric acid was obtained from GFS Chemicals or EMD Chemicals (PX0397 Omni Trace). Ultra high purity research grade oxygen, nitrogen and hydrogen were employed. The counter electrode (CE) was high surface area Pt gauze and the reference electrode (RE) was an in-house constructed reversible hydrogen electrode (RHE). The working electrode (WE) was a glassy carbon ( $\Phi 5 \text{ mm}$ ) substrate on which various catalyst ink dispersions were deposited. Cyclic voltammetry and hydrodynamic voltammetry were carried out using a potentiostat (HZ-3000, Hokuto Denko) and rotating disk electrode set-up (HZ-301, Hokuto Denko).

#### 2.3.2. Measurement of CVs and IVs

Cyclic voltammetry (CV) was carried out in electrolytes saturated with nitrogen and measurements conducted under a  $\text{N}_2$  atmosphere. The electrode was conditioned by cycling for about 20–30 cycles prior to recording data. To obtain a CV, the working electrode was cycled between 0 and  $1100 \text{ mV vs. RHE}$  at  $50 \text{ mV s}^{-1}$  for 3 cycles, and a steady-state cyclic voltammogram based on the third cycle recorded for analysis.

Hydrodynamic voltammetry for the oxygen reduction reaction (ORR) evaluation was conducted by applying linear sweep voltammetry (LSV) under an oxygen atmosphere after saturating the electrolyte for at least 30 min with an oxygen purge. LSVs were recorded for voltage sweeps from 200 to  $1200 \text{ mV}$  using scan rates of  $10 \text{ mV s}^{-1}$ . Care must be taken if staircase voltammetry is employed in terms of selection of the step height, width and

alpha. Rotation speeds of 2000, 1600, 1200, 800, 400 rpm were sequentially imposed. Prior to the LSV at each rotation speed, the electrode was polarized at 50 and  $1100 \text{ mV}$  alternately to construct a reproducible Pt surface. The background currents was also measured under identical protocols to the LSV for ORR while imposing a  $\text{N}_2$  atmosphere; these were later subtracted from the ORR LSVs to account and correct for the charging currents at a given scan rate.

#### 2.3.3. Durability measurements

For durability tests, initial or beginning of life (BOL) diagnostics (CV and LSV) were conducted as explained above after which the atmosphere was switched from oxygen to nitrogen. Subsequently, potential cycles were carried out for 7200 cycles using a rectangular wave profile from 600 to  $1000 \text{ mV vs. RHE}$  with a hold at each potential step for 1 s resulting in 2 s per cycle or 0.5 Hz. The choice of the voltage range was based on two factors: the change of Pt surface from an oxide-free surface at  $600 \text{ mV}$  to an oxide-covered surface at  $1000 \text{ mV}$  as well as the practical consideration of the largest and most detrimental cycle in an actual fuel cell for automotive applications. The number of cycles had to be limited to 7200 since contamination and occasional flaking of catalyst particles from the electrode tip posed an issue after 6–8 h of operation of the experimental set-up. Finally, the gases were switched back from nitrogen to oxygen and end of life (EOL) diagnostics (CV and LSV) were conducted by the same method as initial diagnostics. The BOL and EOL ECA values as well as catalyst activity were compared to estimate the losses incurred during potential cycling.

#### 2.3.4. Reaction order and activation energy measurements

After obtaining steady-state CV under nitrogen, LSV was conducted under 25%, 50%, 100% oxygen concentrations with the balance being nitrogen. LSV ranges extended from 200– $1200 \text{ mV}$  at  $10 \text{ mV s}^{-1}$  and a single rotation speed of 1600 rpm was employed. Using the expression  $I_k = i \times i_L / (i - i_L)$  equation the kinetic current  $I_k$  was calculated. The reaction order was subsequently determined from the slope of  $\log i / \log p\text{O}_2$  plot.

In order to investigate effect of temperature, the ORR activity was evaluated at cell temperatures of 25, 40, 50 and  $60^\circ\text{C}$ . The RHE potential and reversible oxygen potential were corrected for temperature effects. The value of the activation energy ( $\Delta H$ ) for the ORR was determined subsequently from Arrhenius plots.

## 3. Results and discussion

### 3.1. TEM, XRD and CO chemisorption characterization

Dry Pt/C catalyst powders obtained from the catalyst manufacturer (TKK, Japan) were first analyzed using TEM as described in the experimental section. Fig. 1 shows TEM micrographs for baseline Pt/C, Pt/C-HT and PtCo/C along with the particle size distribution based on  $\sim 300$  particles. The particle size distributions are fairly narrow and the average particle size obtained for the baseline Pt/C was estimated to be  $\sim 2.5 \text{ nm}$ , whereas it was much higher at  $4 \text{ nm}$  for the Pt/C-HT. This is expected since heat treatment at high temperatures causes sintering and hence results in particle size growth. Based on simple geometric considerations of the surface area of a sphere, its volume, and the density of Pt, we can write the equation: surface area ( $\text{m}^2 \text{ g}^{-1}$ ) =  $[6/\rho d] = [279/d]$  where  $\rho$  is the density of Pt and  $d$  is the particle diameter in nm. A  $2.5 \text{ nm}$  particle (baseline Pt/C) would correspond to a specific surface area of  $\sim 110 \text{ m}^2 \text{ g}^{-1}$  and a  $4 \text{ nm}$  particle (Pt/C-HT) would have a specific surface area of  $\sim 70 \text{ m}^2 \text{ g}^{-1}$ .

Table 1 is a summary of the characterization of the original dry catalyst powders using various techniques including XRD, TEM, BET and CO chemisorption. One of the most widely used techniques for determination of surface area of catalyst powders is the so-called

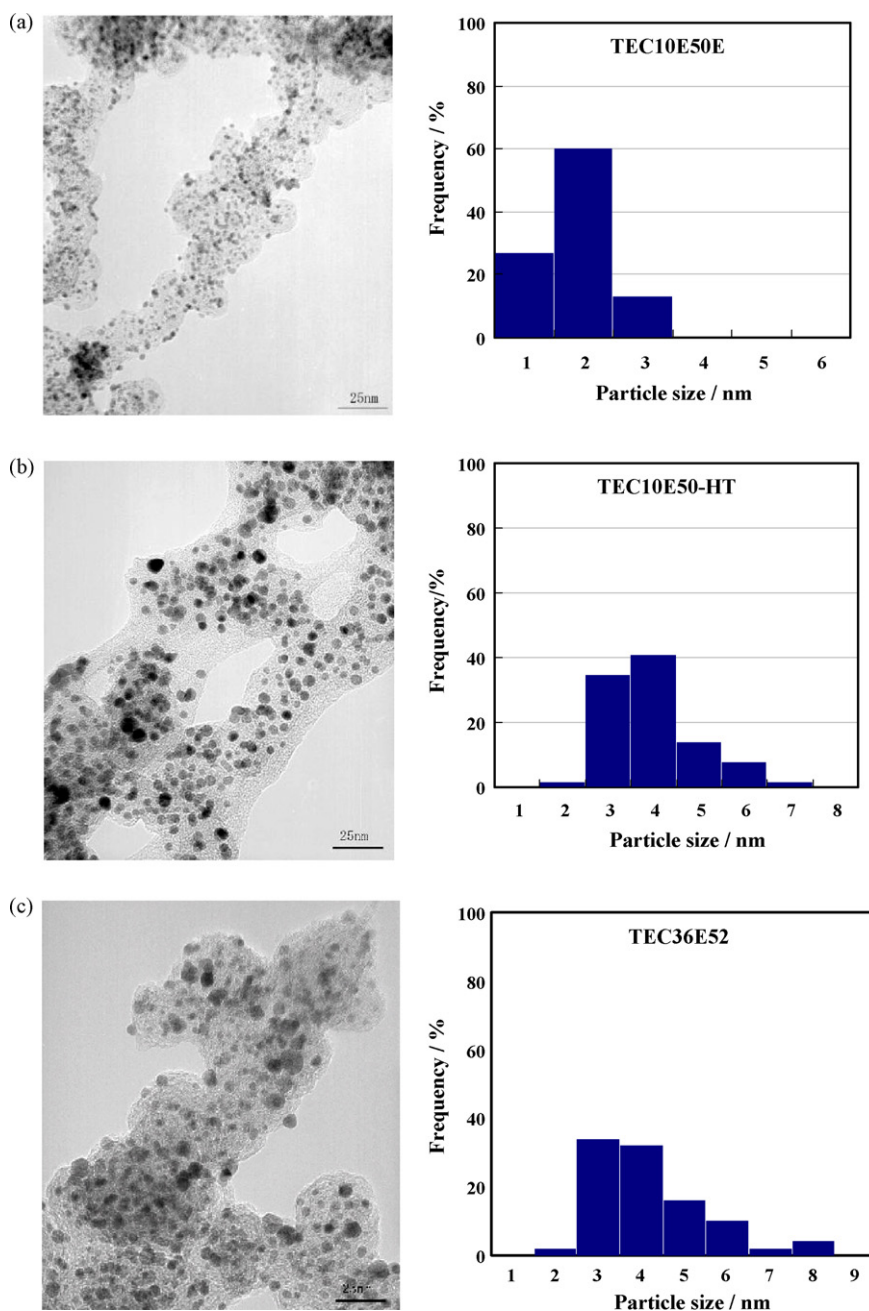


**Fig. 1.** TEM images for the various catalysts (original dry powders) evaluated in this paper along with their particle size distributions (a) 50 wt.% Pt/C, (b) 50 wt.% Pt/C-HT and (c) 50 wt.% PtCo/C.

BET method (Brunauer, Emmett and Teller, 1938). BET measurements using nitrogen adsorption provides us with the total area of Pt and carbon. CO chemisorption estimates allow us to selectively separate the surface area of Pt from carbon and provides another estimate of the total Pt surface area. It should be noted that the area estimated using CO chemisorption is a function of the analysis method and assumptions of the manner in which CO binds to Pt atoms.

### 3.2. Ink formulation and optimization

A review of the literature reveals that optimization of the catalyst ink sprayed or coated onto MEAs of fuel cells is often carefully studied and reported but rarely so in the case of TF-RDE half-cell studies. Often a simple dispersion of Pt/C and water and sometimes ionomer are stirred or mixed to form the ink slurry without any attempt at experimenting with the quality of the dispersion formed

**Table 1**

Specification of the Pt-based carbon supported catalysts (original dry powders) used in formulating inks and TF-RDEs.

Sample	Pt loading (wt.%)	Crystallite size XRD (nm)	Particle size TEM (nm)	Cat surface area BET ( $\text{m}^2 \text{g}^{-1} \text{cat}$ )	Pt Surface area CO ( $\text{m}^2 \text{g}^{-1} \text{Pt}$ )
TEC10E50E (Pt/C)	46	2.4	2.3	311	132
TEC10E50-HT (Pt/C-HT)	50	4.6	5.0	365	78
TEC36E52 (PtCo/C)	46.5	4.3	5.3	–	–

[11,22]. Of all the components in the ink, the ionomer content for TF-RDE studies is not critical since there is an excess of liquid acid electrolyte to provide wetting of the catalyst surface and pores and provide more than sufficient protonic conduction; in fact the principal role of the ionomer is to act a mild glue and prevent flaking off of the electrode under high speed rotation in the electrochemical cell over time. But the composition of other components of the ink such as the water and alcohol (or organic) content as well as the duration of ultrasonication can be extremely important. Several organic compounds may be used with water in the mixture to enhance the dispersion as long as they do not contaminate the catalyst surface or change the viscosity considerably. We report here mainly on a series of tests employing varying isopropanol (IPA) and water content as well as ultrasonication times. The inks were deposited as TFEs and cyclic voltammograms were measured to estimate the under potentially deposited hydrogen (HUPD) or hydrogen adsorption (HAD) charge on the Pt surface to obtain the electrochemical area (ECA,  $\text{m}^2 \text{g}^{-1}$ ).

We examine a couple of cases in detail to highlight the importance of producing a good dispersion with the catalyst ink before depositing it as an electrode. A good dispersion can be qualitatively identified by ultrasonication of the ink and then allowing the ink to sit without stirring for a period of time. We find in our work that some of the good dispersions do not settle or coagulate for many hours and even days while extremely poor dispersions settle in minutes. The final quantitative parameter that we used to decide if the dispersion was optimal was the ECA measured. In the studies reported here, the IPA/total volume ratio was varied systematically in the range 0–50%. Fig. 2 shows the trends observed in the magnitude of the ECA with composition of ink. In the case of the baseline Pt/C we observe an increase in the ECA from 80 to  $100 \text{ m}^2 \text{g}^{-1}$  (25% increase) whereas for the Pt/C-HT an increase from 35 to  $74 \text{ m}^2 \text{g}^{-1}$  (111%) was observed. In the case of the baseline Pt/C, the original catalyst powder is not particularly hydrophobic and thus it was found to be only moderately sensitive to the IPA content and fairly easy to form a good dispersion. The Pt/C-HT original catalyst powder is somewhat hydrophobic (due to its heat treatment) and at low IPA contents, it was difficult to wet and form a good dispersion. A surprising artifact is the decrease in ECA as the IPA content was raised beyond 40%. This decrease was carefully studied and found to be due to the experimental difficulty in accurately metering and depositing a few microliters of the highly viscous alcohol rich ink uniformly onto the surface of the small TF-RDE area. All electrodes were observed under a microscope after drying to confirm that the films deposited were uniform.

The energy and duration of dispersion of the catalyst in IPA and water to form an ink was found to be important. For a given ink composition, ultrasonication times of less than 5 min were

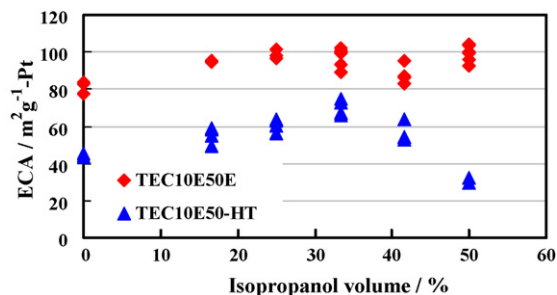


**Fig. 2.** ECA ( $\text{m}^2 \text{g}^{-1}$ ) values plotted as a function of isopropanol content for different ink compositions (Pt/C+water+isopropanol). The inks were used to prepare TF-RDEs and ECA measured in 0.5M  $\text{H}_2\text{SO}_4$ . The ECA shows a pronounced peak in magnitude for about 35% IPA composition for the Pt/C-HT and Pt-alloy/C whereas the peak is rather shallow for the Pt/C baseline catalyst. All inks had identical ultrasonication times of 30 min.

found to produce irreproducible results, and durations greater than 10–15 min were found to be sufficient for all catalysts studied so far. Beyond 15 min and for up to a period of 3 h, the effect of continued ultrasonication was found to produce no observable degradation of the Pt/C catalyst in terms of a loss in ECA or particle growth in TEM indicating a reasonably strong adhesion of Pt to the carbon support.

Based on these results, the optimum ink compositions based on the highest ECA measured were utilized for a comprehensive study of catalyst activity and durability. We must mention here that in order to determine the optimum ink composition for a new unknown catalyst one would need to systematically go through the entire procedure and arrive at a composition that produces the highest ECA. The existing database of catalysts and knowledge of its (Pt or carbon) hydrophobic nature will provide a guideline and precedent for optimizing the composition but there are no shortcuts.

### 3.3. Catalyst activity

In the measurement of catalyst activity, our goal is to obtain a value of activity that is as free of mass-transport effects as possible. In order to obtain an accurate value of the catalyst activity, we make every attempt to measure the current in a regime where ORR kinetics dominate and any residual mass-transport present can be calculated and used to make corrections to obtain a purely kinetic current  $i_k$ . The methodology used for ink preparation reported in the previous section was used to prepare TF-RDEs and subsequently tested in well-cleaned electrochemical cells with the appropriate electrolyte. In Fig. 3(a and b) the basic methodology used for measuring and analyzing the ORR activity in TF-RDE experiments has been illustrated. The method used is similar to that reported in the literature [7,9,23] and involves acquiring linear sweep voltammograms (LSVs) or current–voltage ( $I$ – $V$ ) curves under  $\text{O}_2$  at multiple controlled disk rotation speeds.

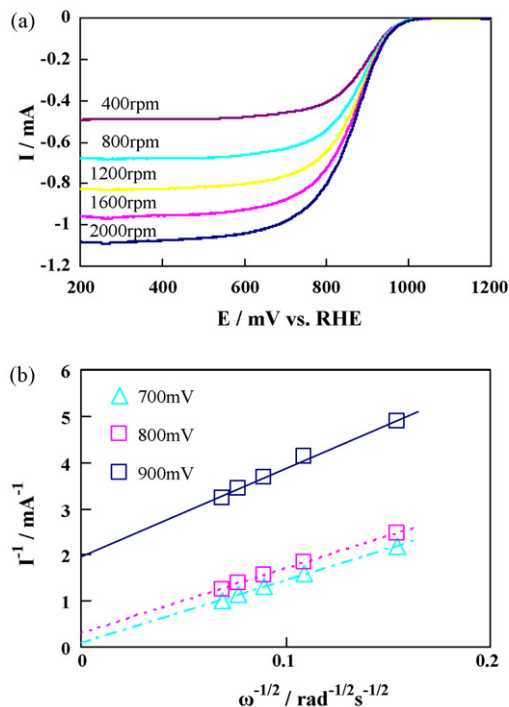


**Fig. 3.** (a) Raw  $i$ – $E$  data obtained from RDE tests for TEC10E50E at 25 °C in sulfuric acid at 400, 800, 1200, 1600 and 2000 rpm. (b) Procedure used in the analysis of  $i$ – $E$  data to obtain kinetic current densities  $i_k$ , i.e., Koutecky–Levich plots at 0.7, 0.8 and 0.90 V.

An important experimental parameter in the experiments is the potential scan rate that is often chosen to be in the range  $1\text{--}50\text{ mV s}^{-1}$  in the literature. The effect of scan rate is a fairly complex issue since at different scan rates, the coverage of Pt with oxides will vary. A study of a large number of experimental protocols that includes the effect of scan rates and oxide coverage will be reported in a separate manuscript elsewhere. The scan rate selected for this work was  $10\text{ mV s}^{-1}$ . A “background scan” at  $10\text{ mV s}^{-1}$  using nitrogen purged electrolyte (instead of oxygen) was carried out and subtracted from the  $\text{O}_2$   $I$ - $V$  curve to eliminate and correct for the effect of pseudo-capacitive currents.

We digress at this point to discuss the utility of measuring catalyst activity in TF-RDE set-ups under controlled sweep rates. Measurements in RDE set-ups are susceptible to contamination from impurities both from the experimental glassware, trace amounts of  $\text{Cl}^-$  in the perchloric acid electrolyte as well as generation of  $\text{Cl}^-$  over time due to decomposition of the acid itself. The technique is thus limited to short-term testing ranging up to a few hours at the most to ensure reproducibility and validity of data. This is one of the justifications for invoking a reasonable potential scan rate of  $5\text{--}50\text{ mV s}^{-1}$  (with corrections for the baseline charging currents).

Of equal import is fact that the oxide species on the Pt surface initially grows very rapidly, followed by a very slow process that is logarithmic in time. A true steady-state condition for a Pt surface in terms of oxide coverage, oxide species and oxide structure are not definable at this time for the measurement of activity since the surface of Pt-based catalysts is not invariant during electrochemical measurements. There is much work to be done to understand the nature of the oxide species and its structure at the Pt surface as a function of potential and time. It should be noted that for Pt/C electrocatalysts employed in subscale PEMFCs data is often acquired at  $\sim 10$  min per point although it is in a pseudo-steady-state [8]. The voltage at constant current continues to fall over a several hours and the phenomenon is often referred to as “reversible decay” since it can be recovered when the catalyst surface is reduced. Ideally, one would recommend that the catalytic activity be reported for a well-defined surface coverage with known oxide species and structure. In practice, the best one can do is to measure the  $I$ - $V$  curves using identical standard measurement protocols (to maintain similar oxide coverage) so that activity results can be compared between laboratories.

We note that the activity of Pt/C measured in the range  $5\text{--}50\text{ mV s}^{-1}$  in flooded TF-RDEs incidentally happens to have a similar magnitude to that measured in un-flooded practical PEMFC electrodes at  $\sim 10$  min per point [8]. Notwithstanding this result, the magnitude of catalyst activity obtained from RDE measurements only provides relative trends rather than absolute values. The RDE technique is meant to be applied as a rapid screening tool for newly developed fuel cell catalysts available in mg quantities. With such small quantities of laboratory-synthesized catalysts, it is not possible to measure the activity in MEAs that require a few grams for preparation and testing. Hence, most automotive companies as well as national laboratories and universities involved in the US DOE hydrogen program carry out investigations of new catalyst materials using the thin-film RDE technique described in this paper.

On completion of the CVs,  $I$ - $V$ s and background experiments, we plot  $I^{-1}$  vs.  $\omega^{-1/2}$  (Koutecky–Levich or  $K$ - $L$  Plot) as shown in Fig. 3. The intercept extrapolated to infinite rotation speed is then extracted and finally a plot of  $\log i_k$  vs.  $V$  also known as the Tafel plot is derived. We note that in our results (as well as that reported in the literature), there is a significant deviation from a Tafel slope of  $70\text{ mV dec}^{-1}$  in the high current density regime that researchers refer to as the “double Tafel regime”. This double Tafel is often attributed to the change in kinetics caused by lower oxide coverage

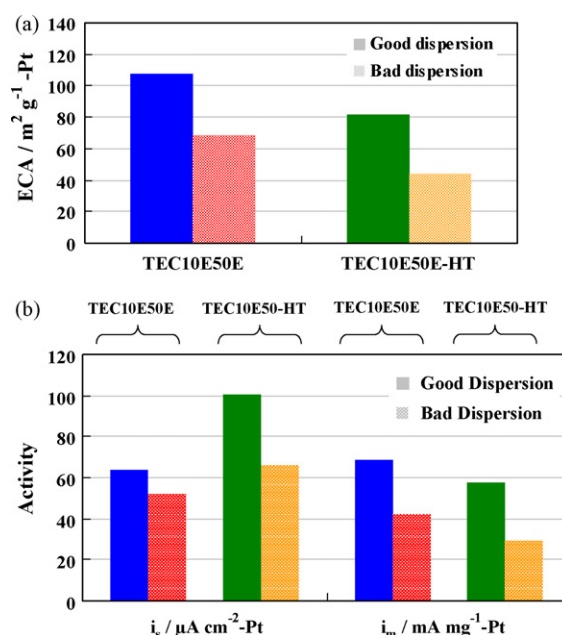


**Fig. 4.** (a) ECA for the baseline Pt/C and heat treated Pt/C-HT when measured using the optimum ink formulation (good dispersion: 35% IPA) and compared to that for a poor dispersion: 10% IPA and (b) illustrates the corresponding values for specific activity  $i_s$  and mass activity  $i_m$ . A significant increase in ECA as well as activity is obtained for the well-dispersed catalysts. Errors in the determination of  $i_s$  and  $i_m$  are likely if the ink formulation is not well-dispersed.

and different controlling adsorption isotherm at lower potentials. The correction factor involved in going from the raw  $I$ - $V$  curves to the Tafel plots,  $i_k$ - $V$ , corrected by Koutecky–Levich equation is considerable with the typical correction being about 40% even at high potentials (low currents) of 900 mV and extremely high in the high current region of the first Tafel regime. The corrections required to be made to the  $I$ - $V$  curve become extremely high at lower potentials and we think speculation about the relation between the double Tafel slope and kinetic factors causing it is debatable. Since we are primarily interested in the kinetic regime,  $K$ - $L$  corrected kinetic currents  $i_k$  at 900 mV is a good and accepted measure of the ORR activity of the catalyst. The specific activity  $i_s$ , is derived by normalizing kinetic currents  $i_k$ , by the electrochemical area, ECA, measured from HUPD of CVs and the mass activity  $i_m$ , obtained by normalizing to the loading ( $\mu\text{g cm}^{-2}$ ) of the catalyst applied to the electrode.

Fig. 4 depicts the ECA and ORR activity ( $i_m$ ) for well-dispersed and poorly dispersed samples in sulfuric acid. When the surface of the Pt is not fully contacted with electrolyte as in the poorly dispersed electrodes, their mass activity can be significantly lower, and in this case it is by a factor of 2. Thus the extra effort expended in optimizing the catalyst ink is demonstrated to be necessary and indispensable to obtain an accurate estimate of the catalyst activity.

Using the optimized ink formulation, the catalysts were evaluated for reproducibility of ECA and ORR activity in both sulfuric and perchloric acid. Fig. 5(a) and (b) shows the reproducibility of the measured ECA and activity for 10 sample electrodes immersed in  $0.5\text{ M H}_2\text{SO}_4$ . The average value of the ECA was found to be  $\sim 105\text{ m}^2\text{ g}^{-1}$ . Further, the ORR activity ( $i_s$ ,  $i_m$ ) for the same catalyst in both acids are reported. The average value of  $i_s$  and  $i_m$  in sulfuric acid are:  $60\ \mu\text{A cm}^{-2}\text{-Pt}$  and  $70\ \text{mA mg}^{-1}\text{-Pt}$  and in perchloric acid are:  $292\ \mu\text{A cm}^{-2}\text{-Pt}$  and  $266\ \text{mA mg}^{-1}\text{-Pt}$ . These values are slightly higher than that typically reported by other researchers for Pt/C catalyst in the literature. Table 2 is a summary of the electrocatalyst activity of catalysts evaluated in this work as well as that reported in the literature.

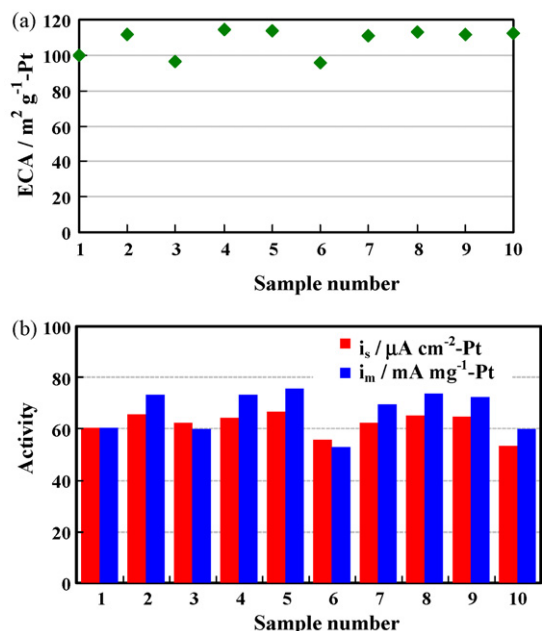


**Fig. 5.** (a) ECA ( $\text{m}^2 \text{g}^{-1}$ ) measured for 10 samples of baseline Pt/C using TF-RDE in 0.5 M sulfuric acid at 25 °C. For baseline Pt/C catalyst, an average value of  $105 \text{ m}^2 \text{g}^{-1}$  was obtained. (b) Reproducibility of ORR activity measurements ( $i_s$  and  $i_m$ ) for baseline Pt/C catalyst in 0.5 M sulfuric acid at 25 °C.

### 3.4. Heat treated Pt/C and PtCo/C

Although the Pt/C baseline is a commonly used catalyst with a very high activity, alternative catalysts such as Pt/C-HT as well as PtCo/C are being considered for use in PEMFCs. These catalysts provide either a higher activity or higher durability or both that is much needed for commercialization of PEMFCs for automotive use. Since both these catalysts are heat treated, they have a larger particle size of  $\sim 4 \text{ nm}$  and hence a lower value of the ECA. Fig. 6 presents the ECA, specific activity and mass activity of the three catalysts in 0.1 M HClO<sub>4</sub>. The baseline Pt/C catalyst exhibited the highest surface area due to its small particle size and moderate mass activity whereas the PtCo/C alloy catalyst showed the lowest area with the highest specific and mass activity. Pt/C-HT as well as the PtCo/C exhibited lower electrochemical surface areas due to the particle size growth caused by annealing at high temperatures. The higher activity of the Pt-alloy catalyst has been ascribed to the negative shift in the d-band center for PtCo/C [26]. This negative d-band center shift leads to a lower adsorption of both blocking species and reaction intermediates. Fig. 7 shows the magnification of the

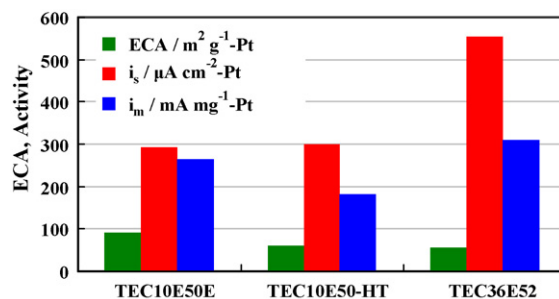


**Fig. 6.** ECA, specific activity  $i_s$  and mass activity  $i_m$  for 3 Pt-based catalysts (Pt/C, Pt-HT/C and PtCo/C) measured using optimum ink formulations in 0.1 M perchloric acid at 25 °C. The PtCo/C shows a lower ECA, a significantly higher specific activity (1.8×) compared to the baseline Pt/C and a slight enhancement of mass activity.

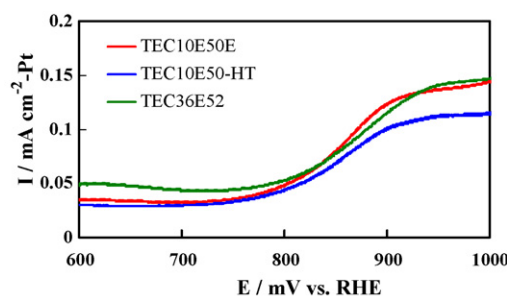


**Fig. 7.** Magnification of the onset of oxide formation for the 3 catalysts shown in the oxidation sweep (600–100 mV) of the CVs. The onset of oxide formation for Pt-HT/C and PtCo/C is observed to be shifted to positive potentials compared to baseline Pt/C.

onset of oxide formation on the 3 catalyst in the oxidation sweep of the CVs. The onset of oxide formation for Pt-HT/C and PtCo/C is shifted positively indicating lower amount of intermediates that act as adsorbed blocking or spectator species and impede the ORR reaction. For PtCo/C, evidently the lower adsorption of blocking species leads to improved ORR activity as has been reported previously in the literature. This shift in the onset can thus be used as a secondary indicator for an improved activity catalyst.

### 3.5. Anion adsorption effects on activity

We find that (Fig. 5b) the average value of the activity of baseline Pt/C is  $\sim 65 \mu\text{A cm}^{-2} \text{Pt}$ ; on the other hand (Fig. 6) the specific activity of baseline Pt/C in 0.1 M HClO<sub>4</sub> is  $\sim 292 \mu\text{A cm}^{-2} \text{Pt}$  revealing the strong effect that anion adsorption of SO<sub>4</sub><sup>2-</sup> can have on  $i_s$  and  $i_m$ . Since results in the literature are performed in different acids as

**Table 2**

Summary of the electrocatalytic activity of Pt-based carbon supported catalysts evaluated in this work and comparison to the literature.

Method	Sample	T (°C)	Electrolyte	d (nm)	$i_s$ ( $\mu\text{A cm}^{-2} \text{Pt}$ )	$i_m$ ( $\text{mA mg}^{-1} \text{Pt}$ )	Sweep rate ( $\text{mV s}^{-1}$ )	Reference
TF-RDE	46% Pt/HSC (TKK)	25	0.5 M H <sub>2</sub> SO <sub>4</sub>	2.0	56	56	10	This work
TF-RDE	46% Pt/HSC (TKK)	25	0.1 M HClO <sub>4</sub>	2.0	292	266	10	This work
TF-RDE	46% Pt/HSC (TKK)	25	0.5 M H <sub>3</sub> PO <sub>4</sub>	2.0	29	28	10	This work
TF-RDE	40% Pt/Vu (E TEK)	25	0.1 M HClO <sub>4</sub>	–	190	69	5	[8]
TF-RDE	40% Pt/Vu (E TEK)	25	0.1 M HClO <sub>4</sub>	–	310	110	20	[8]
TF-RDE	45.9% Pt/HSC-E (TKK)	25	0.1 M HClO <sub>4</sub>	–	190	160	5	[8]
TF-RDE	45.9% Pt/HSC-E (TKK)	25	0.1 M HClO <sub>4</sub>	–	240	200	20	[8]
TF-RDE	20% Pt/Vulcan	60	0.5 M H <sub>2</sub> SO <sub>4</sub>	3.0	35	–	5	[7]
Macro-homogeneous model	20% Pt/C (E TEK)	20	0.5 M H <sub>2</sub> SO <sub>4</sub>	–	7	–	5	[24]
Porous RDE	10 wt.% Pt/Vulcan XC72	25	1.0 M H <sub>2</sub> SO <sub>4</sub>	1.8	11	17	1	[25]
UMEC + Nafion	10 wt.% Pt/Vulcan XC72	25	1.0 M H <sub>2</sub> SO <sub>4</sub>	1.8	10	16	1	[25]
UMEC (ultramicroelectrode with cavity)	10 wt.% Pt/Vulcan XC72	25	1.0 M H <sub>2</sub> SO <sub>4</sub>	1.8	8.1	13	1	[25]
TF-RDE	Pt/C (TKK)	20	0.1 M HClO <sub>4</sub>	1–1.5	$\sim 350$	–	20	[9]
TF-RDE	Pt/C (TKK)	20	0.1 M HClO <sub>4</sub>	2–3	$\sim 200$	–	20	[9]
TF-RDE	Pt/C (TKK)	20	0.1 M HClO <sub>4</sub>	5	$\sim 150$	–	20	[9]

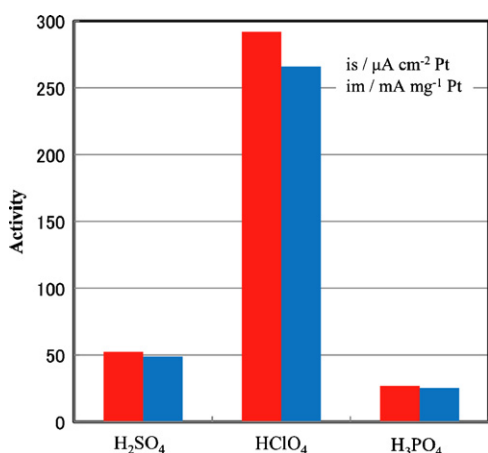


**Fig. 8.** Effect of anion adsorption on the specific and mass activity of baseline Pt/C catalyst. The catalyst activity in the 3 acids follows the trend  $\text{HClO}_4 > \text{H}_2\text{SO}_4 > \text{H}_3\text{PO}_4$ . The activity of baseline Pt/C is about 6 times lower in sulfuric acid compared to perchloric acid as a result of the higher anion adsorption of sulfate ions. Red bars correspond to  $i_s$  and blue bars correspond to  $i_m$ . (For interpretation of the references to colour in this figure legend, the reader is referred to the web version of this article.)

an estimate of the activity of Pt in a fuel cell with Nafion as a membrane, we decided to extend the investigation of the effect of anion adsorption on Pt by evaluating the activity of the Pt/C in phosphoric acid also. Fig. 8 summarizes the activity of baseline Pt/C in all three acids. We observe that the activity of baseline Pt/C follows the trend  $I_{\text{perchloric acid}} > I_{\text{sulfuric acid}} > I_{\text{phosphoric acid}}$  as a result of the strong anion adsorption of phosphate ions that inhibits ORR kinetics. The activity of Pt in perchloric acid most closely resembles that of Pt in the MEA of a fuel cell at least in part due to the low anion adsorption in both Nafion and perchloric acid. Another important fact that is often neglected, in that, although phosphoric acid fuel cells (PAFCs) have several advantages over PEMFC in terms of high temperature operation and water management, they show a significant activity loss due to strong adsorption of phosphate ions on Pt. Fig. 9a depicts the superimposed cyclic voltammograms in the three acids and Fig. 9b shows a magnification of the voltage regime where onset of oxide commences. The HUPD (Fig. 9(a)) observed in phosphoric acid is comparable to that in sulfuric acid and higher than that in perchloric acid. We note though that in the HUPD region, the anion adsorption results in a superimposed peak that enhances the weakly adsorbed  $H_{\text{ads}}$  peak; this can lead to a slight overestimate of the calculated ECA. The estimates of ECA from sulfuric acid thus are slightly higher than that obtained from perchloric acid. A magnification of the CVs (Fig. 9(b)) measured in perchloric, sulfuric and phosphoric acid in the potential range 600–1000 mV, reveals that the onset of oxide species formation shifts towards positive potentials by as much as 220 mV with the trend perchloric acid < sulfuric acid < phosphoric acid. The importance of this artifact in terms of using TF-RDE to test catalysts for fuel cells is that the onset of oxides in sulfuric acid is much closer to that in Nafion. Since the onset of oxides partially determines the stability of the catalyst under potential cycling, sulfuric acid appears to be a better candidate for carrying out simulated fuel cell durability tests.

### 3.6. Catalyst utilization

Although the primary purposes in carrying out thin-film RDE experiments are the screening of small quantities of new catalysts for PEMFCs for surface area, catalytic activity and relative durability rates, the electrochemical area (ECA) can also be used to estimate the utilization of the catalyst both in the TF-RDE experiments as well as in MEAs of actual fuel cells. The particle size of the original dry catalyst powder was measured using the varied techniques of

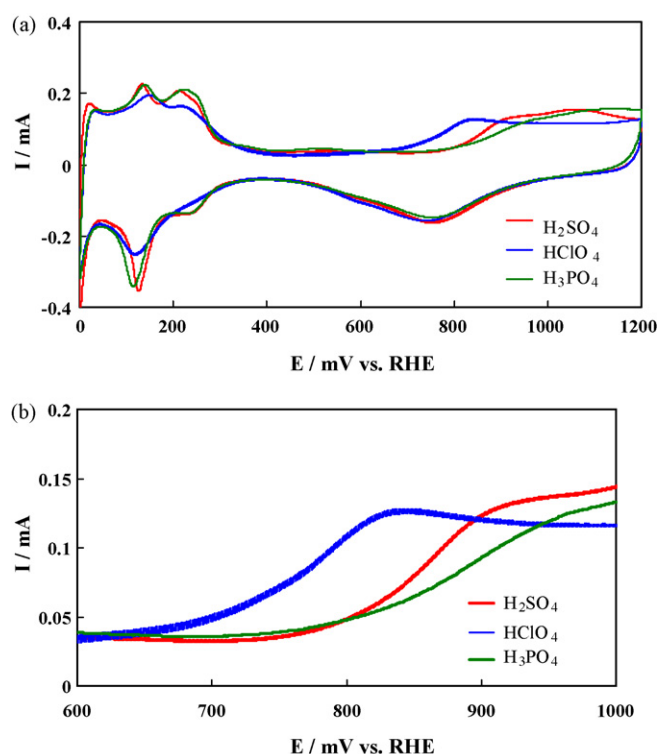


**Fig. 9.** (a) Entire CV for Pt/C in perchloric, sulfuric and phosphoric acids and (b) magnification of the CVs measured in perchloric, sulfuric and phosphoric acid in the potential range 0.60–1.0V illustrating the shift in the onset of oxides.

TEM, XRD and CO chemisorption (see Table 1). Each of these very different techniques provides us a slightly different insight into the nature of the catalyst powder. Nevertheless, the average particle size for a catalyst determined using these techniques agree with each other within error. The values obtained from these techniques can be assumed to be an upper limit of the catalyst surface area available in the original dry powder before it is processed either to prepare TF-RDE electrodes or MEAs for fuel cells.

The ECA measured in liquid electrolytes from CVs is based on the under potential hydrogen (HUPD) adsorbed on the Pt surface. The ECA thus measures all of the catalyst that is in contact electronically to the carbon and the electrode while simultaneously in contact with protons from the acid electrolyte or membrane of fuel cells. In liquid electrolytes it is expected that except in very small pores that are not filled with electrolyte a protonic path to almost all the Pt sites exists. In addition, small losses are expected from the dissolution of very small particles that are unstable and do not last even a few cycles of potential cycling. Thus comparing the ECA in liquid electrolytes to the particle size obtained from original dry powders gives us the first level of utilization that is reported to attain quite high values of around 80%. Unlike studies in liquid electrolyte where there are abundant protonic paths, in MEAs of fuel cells, the catalyst in the electrode layer is in contact with carbon and a limited amount of ionomer. The ratio of ionomer to carbon or I/C becomes an important parameter since a suboptimal amount of ionomer results in poor contact and an excess of ionomer results in plugging of the electrode pores causing poor mass-transport. Pt utilization in the catalyst layer needs to be maximized to minimize the cost of fuel cells. In order to obtain a measure of Pt utilization in MEAs, the ratio of the ECA in liquid electrolytes to that measured *in situ* in a fuel cell is invoked.

Fig. 10 is a plot of the catalyst utilization when compared to areas measured under CO chemisorption, liquid electrolyte, and *in situ* in MEA. We observe that the in-house MEAs, prepared for this work



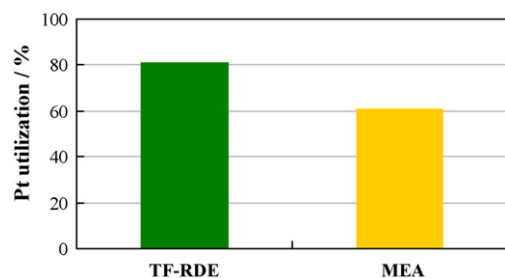


**Fig. 10.** Pt surface area measured in TF-RDE in perchloric acid and in MEAs using Nafion membrane. The utilization of Pt is quite high in MEAs at about 75% in relation to the values obtained from TF-RDE where complete contact between liquid electrolyte and catalyst surface is expected.

and also reported elsewhere in more detail, exhibit a fairly high utilization of ~75% (compared to utilization in RDE/liquid electrolyte where all accessible catalyst particles are assumed contacted by protons) indicating that the ionomer/carbon ratio is reasonably close to the optimum. Further complex measures of catalyst utilization under actual fuel cell operation involve the usage of Pt along the thickness of the cathode catalyst layer (usually about 5–10  $\mu\text{m}$ ) at varying current densities and is out of the scope of the present discussion.

### 3.7. ORR reaction order and activation energy

In actual practice, TF-RDE measurements are carried out by researchers under various arbitrary conditions as was shown in Table 2. In addition to providing a reproducible method and a benchmark, we now examine the effect of temperature and pressure so that simple conversions can be made for comparisons of results obtained under different operating conditions by different research groups.

The reaction order is generally defined as the rate of change of activity with partial pressure. One of the original definitions of the reaction order for ORR was stated by Vetter [27] as:  $\log(i)/\log(p\text{O}_2)$  at constant potential  $E$ , which we refer to as “ $m$ ” or the “total reaction order”. Several other definitions for the reaction order and their interrelations are well-elucidated in the classic text by Gileadi [28]. Two other reaction orders often invoked are the “kinetic reaction order”:  $\log(i)/\log(p\text{O}_2)$  at constant overpotential  $\eta$  and  $\log(E)/\log(p\text{O}_2)$  at constant current. The total and kinetic reaction orders are related by the expression  $\gamma = m - 1/4$  for an assumed transfer co-efficient of  $\alpha = 1$ .

Discrepancies exist between the values of the reaction order of the ORR reported in MEAs and that reported in TF-RDE measured in liquid electrolytes that have not been discussed or treated in the literature. Table 3 summarizes the literature values of reaction order in PEMFCs and liquid electrolytes. The reaction order typically reported from experiments conducted in liquid electrolytes is the kinetic reaction order “ $\gamma$ ” at constant overpotential “ $\eta$ ”; this has often been reported to be 1 (see Table 3) implying that  $m = 1.25$ . In actual PEMFCs where Nafion or similar perfluorosulfonic acid polymer is used as electrolyte, the typically reported reaction order “ $m$ ” at constant potential  $E$  has been reported to be ~0.80 by several

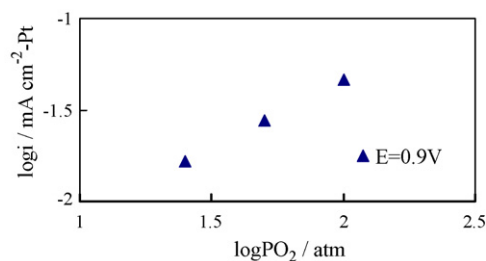


**Fig. 11.** Log–log plot of the kinetic current at  $E = 0.90 \text{ V}$  vs. partial pressure of oxygen with the slope defined as the reaction order ‘ $m$ ’ at constant potential. The reaction order was found to be 0.75.

groups implying that the kinetic reaction order  $\gamma \sim 0.55$  [18,19]. We note that in MEAs of PEMFCs, data is acquired under pseudo-steady-state conditions that may vary from 5 to 15 min per data point whereas in RDE a sweep rate of 1–50  $\text{mV s}^{-1}$  is employed. A possible source leading to the observed discrepancy may be the protocol used to measure the  $I$ – $V$  curve under  $\text{H}_2|\text{O}_2$  which is known to affect the surface oxide coverage of Pt and in turn the measured catalyst activity. The coverage of Pt surface with oxide species might in turn be expected to affect the reaction order itself. Taking these considerations into account, the reaction order in RDE was measured two different ways in our work: under typical RDE sweep rates of 10  $\text{mV s}^{-1}$  and also under steady-state constant potential conditions of 10 min per point preceded by a pre-treatment or pre-conditioning voltage-hold step to grow a controlled and defined amount of oxide species before each measurement.

The reaction order experiments were carried out by purging and saturating the electrochemical cell with  $\text{O}_2/\text{N}_2$  gas mixtures of desired combinations. Fig. 11 is a log–log plot of the kinetic current vs. partial pressure of oxygen using typical RDE sweep measurements; the kinetic reaction order was determined to be ~0.5. Under steady-state potential hold conditions, the reaction order  $m$  at constant potential was found to be ~0.80 after higher oxide coverage pre-treatment and ~0.70 after low oxide coverage pre-treatment, the average of which is ~0.75. These results imply that the kinetic reaction order  $\gamma = m - 1/4$  at constant overpotential  $\eta$  is about 0.50. Our results for the value of  $m$  match the results of tests conducted in MEAs of PEMFCs reported in the literature. Our current study was not sensitive enough to discern clear differences of reaction order on ‘oxide-covered’ and ‘oxide-free’ surfaces partly because our activity point is defined at 900 mV where oxides grow during the potential hold related to the measurement itself. This discrepancy between MEA and RDE results for reaction order does not exist in our results, and the reasons for the higher value of  $\gamma = 1$  reported for Pt in TF-RDE liquid electrolytes in the literature cannot be explained at this time.

This study of reaction order was conducted partly in order to apply the value to estimate the activation energy  $\Delta H$  from Arrhenius plots and thus be able to convert the measured catalyst activity value to a different pressure and temperature. The same electrochemical cell incorporating a water bath for heating was used to measure the ORR kinetics at different temperatures. The ORR experiments were conducted at 25, 50, and 70  $^\circ\text{C}$ . Fig. 12 shows the Arrhenius plot, the slope of which is the activation energy

**Table 3**  
Summary of results and comparison to the literature values of ORR reaction order (‘ $m$ ’ at constant potential and ‘ $\gamma$ ’ at constant overpotential) in liquid acid electrolytes.

Electrode	$m$	$\gamma$	Range	Electrolyte	Reference
TEC10E50-HT thin-film	0.75	0.5	$E = 0.9 \text{ V}$ vs. RHE	0.5 M $\text{H}_2\text{SO}_4$	This work
Pt	1/2, 1	–	High current region, low current region	1N $\text{H}_2\text{SO}_4$	[21]
Pt	1	–	Tafel region	0.1 M $\text{HClO}_4$	[16]
PBI or Nafion thin-film on Pt	0.7–0.9, 0.3–0.5	–	Bare Pt, oxide-covered Pt	0.1 M $\text{HClO}_4$ , 0.1 M $\text{H}_2\text{SO}_4$ , 0.1 M $\text{H}_3\text{PO}_4$	[20]
Pt/Vulcan thin-film	$1.00 \pm 0.05$	–	ca. 745–845 mV	0.5 M $\text{H}_2\text{SO}_4$	[7]

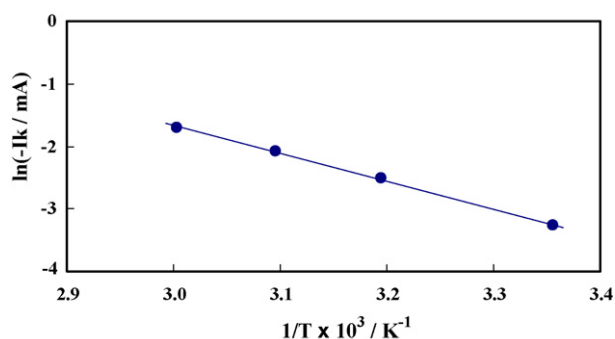


**Fig. 12.** Arrhenius plot of the kinetic current  $i_k$  vs. the inverse of absolute temperature. The slope of plot is the activation energy and determined to be  $38 \text{ kcal mol}^{-1}$ .

and determined to be  $38 \text{ kcal mol}^{-1}$  at constant potential. For this parameter also, results reported in the literature show some scatter as shown in Table 3. Our values fall in the expected range even though we have applied a reaction order of 0.5 (as determined in our experiments) in the calculations for corrections to the concentration of oxygen.

### 3.8. Catalyst durability

PEMFC stacks used for automotive purposes experience hundreds of thousands of load or potential cycles of varying amplitude, frequency and cycle profile [2]. In the automotive industry the distribution of cycles of various profiles is represented by “drive-cycles”. The effect of potential cycling on the catalyst layer of MEAs is now accepted to be one of the most serious challenges to the durability of Pt/C over an expected 10-year life-span. It has thus become imperative to screen new catalyst materials not only for activity but also for short-term durability in order to assess their usefulness. The widest potential range that a fuel cell typically experiences corresponds roughly to the span between peak load and idle which in turn corresponds to potentials of about  $\sim 600$  and  $\sim 950$  mV, respectively. In other unreported work from our group, we have investigated various cycle parameters such as cycle profile and frequency, and found that a square cycle profile results in the highest degradation loss due to Pt dissolution. Based on those results, in this work, we have subjected our catalysts in TF-RDEs to a square cycle profile in the potential range of 600–1000 mV for 7200 cycles having a period of 2 s. As explained in previous section, experimental issues limit us to tests that last less than about 8 h.

As briefly mentioned in the introduction, both perchloric acid and sulfuric acid have been used in the determination of the ORR activity of PEMFC catalysts. Perchloric acid offers low anion adsorption but includes  $\text{Cl}^-$  contaminants both as impurities as well as that generated during experimentation due to its decomposition. Sulfuric acid does not have these issues and is also expected to accelerate the dissolution of Pt due to the formation of complexes thus helping to reduce experimental test time in the RDE apparatus. In addition, Nafion membrane and ionomer in PEMFCs are known to degrade releasing sulfate ions that adsorb on Pt lowering both its activity and durability further justifying experiments using sulfuric acid. We have thus examined the effect of acid type on the durability of the baseline catalyst in addition to determining the relative durability rates of the 3 sample catalysts in our study.

Fig. 13 depicts the loss in ECA and  $i_m$  for the baseline Pt/C catalyst in sulfuric, perchloric and phosphoric acids. We clearly observe that degradation/dissolution of Pt is highest for sulfuric acid and lower for perchloric and phosphoric acids. Sulfuric acid is expected to facilitate the formation of complexes of Pt that proceed to dissolve easily. The percentage loss in ECA for Pt/C in sulfuric acid was the largest at 37% whereas it was 20% in phosphoric and 15% in per-

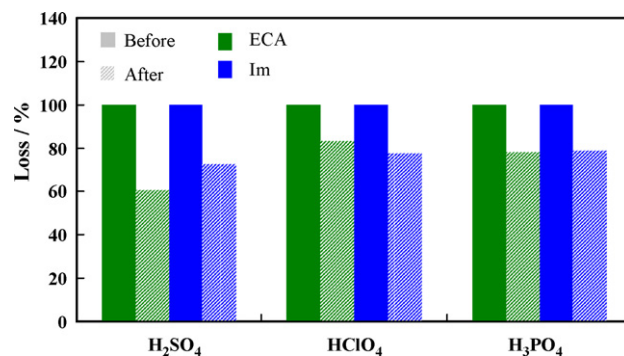


**Fig. 13.** Loss in ECA and  $i_m$  for the baseline Pt/C catalyst in sulfuric, perchloric and phosphoric acids when subjected to potential cycling. The % loss was the greatest in sulfuric acid.

chloric acid. The trend was similar for the mass activity losses. The specific activities remained almost the same before and after the cycling test in all acids since the intrinsic activity of the Pt/C changed very slightly with a small growth in particle size; in some cases a 5% increase in specific activity was observed. Lastly, 3 catalysts including the baseline Pt/C, Pt/C-HT and PtCo/C were all evaluated under the same durability protocol in all three acids. The loss in ECA in perchloric and sulfuric acids are shown in Fig. 14. The heat treated Pt/C:Pt-alloy catalyst/C: baseline benchmark exhibited losses of 39%: 10%: 7%. These results are in qualitative agreement to that reported for practical fuel cells.

Although a detailed discussion of the mechanism and hypotheses for relative dissolution of the different catalysts in this study is not in the scope of this work, we provide a short discussion of the hypothesis based on our work in MEAs of fuel cells as well as the very fundamental work using techniques such as LEED spot profile analysis and STM reported in the literature. During cycling in the range of 600–1000 mV, the Pt surface changes from one covered with oxides to one that is free of oxides. Both the bare Pt and Pt-oxides are susceptible to dissolution. During the first complete cyclic sweep, the irregular islands or mesa-like structures are formed and the displaced less co-ordinated Pt atoms do not go back to their original positions during the reduction sweep. During the next anodic sweep, the atoms at the edges of these islands are obviously more active and susceptible to attack and dissolution. In the case of heat treated Pt, the particle size is larger and the surface is probably akin to the “skin” structures for annealed catalysts reported in the literature. For high surface area heat treated Pt and Pt-alloys on carbon, we suggest a similar mechanism where the surface is more stable due to both, heat treatment that results in less relaxed surface structures, and, in part, due to contribution from the alloying element.

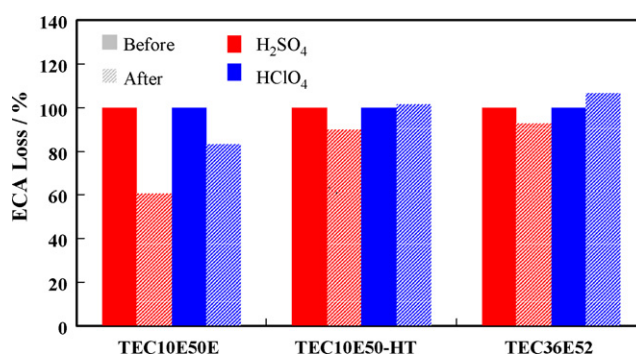


**Fig. 14.** Loss in ECA of baseline Pt/C, Pt/C-HT and PtCo/C catalysts when subject to potential cycling. Over the 7200 potential cycles, the baseline Pt/C showed the highest degradation in ECA.

#### 4. Conclusions

Optimally dispersed inks of platinum dispersed on carbon support were investigated using carefully controlled measurement protocols and well-characterized commercial materials to provide benchmark values for ORR activity and related parameters. The ECA, specific activity and mass activity of baseline Pt/C in perchloric acid was determined. The catalyst activity was shown to be significantly lowered with increased anion adsorption with the order of activity being  $\text{HClO}_4 > \text{H}_2\text{SO}_4 > \text{H}_3\text{PO}_4$ . Perchloric acid has low anion adsorption on Pt and simulates catalytic activity closest in magnitude to values obtained in MEAs using Nafion membrane. The ORR reaction order at constant overpotential was found to be in agreement to that reported in PEMFCs and is about 0.5. This value differs from the values typically reported in the literature for Pt in liquid electrolytes of 1. The activation energy was found to be  $38 \text{ kJ mol}^{-1}$  and falls in the range of values reported in the literature. The values of reaction order and the activation energy may be applied to predict catalytic activity under conditions different from that measured. The durability of the catalysts was evaluated using a voltage cycling protocol that roughly simulates simplified drive-cycle conditions experienced by automotives. The durability of Pt in sulfuric acid was found to be lower than in perchloric acid indicating higher dissolution of Pt in the presence of sulfate ions. The durability measured in the acids increased following the trend:  $\text{H}_2\text{SO}_4 > \text{H}_3\text{PO}_4 > \text{HClO}_4$ .

#### References

[1] M. Uchimura, S. Kocha, ECS Trans. 11 (2007) 1215.

- [2] M. Uchimura, S. Sugawara, Y. Suzuki, J. Zhang, S.S. Kocha, ECS Trans. 16 (2008) 225.
- [3] H.A. Gasteiger, J.E. Panels, S.G. Yan, J. Power Sources 127 (2004) 162.
- [4] T. He, E. Kreidler, L. Xiong, E. Ding, J. Power Sources 165 (2007) 87.
- [5] J.S. Cooper, P.J. McGinn, Appl. Surf. Sci. 254 (2007) 662–668.
- [6] J.F. Whitacre, T.I. Valdez, S.R. Narayanan, Electrochim. Acta 53 (2008) 3680–3689.
- [7] U.A. Paulus, T.J. Schmidt, H.A. Gasteiger, R.J. Behm, J. Electroanal. Chem. 495 (2001) 134.
- [8] H.A. Gasteiger, S.S. Kocha, B. Sompalli, F.T. Wagner, Appl. Catal. B 56 (2005) 9.
- [9] K.J.J. Mayrhofer, D. Strmcnik, B.B. Blizanac, V. Stamenkovic, M. Arenz, N.M. Markovic, Electrochim. Acta 53 (2008) 3181.
- [10] E. Higuchi, H. Uchida, M. Watanabe, J. Electroanal. Chem. 583 (2005) 69.
- [11] J. Maruyama, I. Abe, J. Power Sources 148 (2005) 1.
- [12] D.B. Sepa, M.V. Vojnovic, Electrochim. Acta 26 (1981) 781.
- [13] S.L. Gojkovi, S.K. Zecevic, R.F. Savinell, J. Electrochem. Soc. 145 (1998) 3713.
- [14] M.D. Macia, J.M. Campina, E. Herrero, J.M. Feliu, J. Electroanal. Chem. 564 (2004) 141.
- [15] A. Kuzume, E. Herrero, J.M. Feliu, J. Electroanal. Chem. 599 (2007) 333.
- [16] V. Stamenkovic, N.M. Markovic, J.P.N. Ross, J. Electroanal. Chem. 500 (2001) 44.
- [17] A. Ohma, S. Yamamoto, K. Shinohara, ECS Trans. 11 (2007) 1181.
- [18] H. Xu, Y. Song, H.R. Kunz, J.M. Fenton, J. Electrochem. Soc. 152 (2005) A1828.
- [19] K.C. Neyerlin, W. Gu, J. Jorne, H.A. Gasteiger, J. Electrochem. Soc. 153 (2006) A1955.
- [20] S.K. Zecevic, J.S. Wainright, M.H. Litt, S.L. Gojkovic, R.F. Savinell, J. Electrochem. Soc. 144 (1997) 2973.
- [21] A. Damjanovic, J. Electrochem. Soc. 138 (1991) 2315.
- [22] T.J. Schmidt, H.A. Gasteiger, R.J. Behm, J. Electrochem. Soc. 146 (1999) 1296.
- [23] O. Antoine, Y. Bultel, R. Durand, J. Electroanal. Chem. 499 (2001) 85.
- [24] F. Gloaguen, P. Convent, S. Gambaure, O.A. Velevb, S. Srinivasanb, Electrochim. Acta 43 (1998) 3767.
- [25] E. Guilminot, A. Corcella, M. Chatenet, F. Maillard, J. Electroanal. Chem. 599 (2007) 111.
- [26] V.R. Stamenkovic, B.S. Mun, M. Arenz, K.J.J. Mayrhofer, C.A. Lucas, G. Wang, P.N. Ross, N.M. Markovic, Nat. Mater. 6 (2007) 241.
- [27] K.J. Vetter, Electrochemical Kinetics, Academic Press, New York, 1967.
- [28] E. Gileadi, Electrode Kinetics for Chemical Engineers and Materials Scientists, VCH Publisher, Ltd., London, 1993.